



**Response of the National Ignition Facility
Target Chamber Walls to the Microexplosion
of a Fusion Target**

R.R. Peterson, J.J. MacFarlane, P. Wang

May 1994

UWFDM-952

Prepared for the Eleventh Topical Meeting on the Technology of Fusion Energy, June 19–23, 1994, New Orleans LA.

FUSION TECHNOLOGY INSTITUTE

UNIVERSITY OF WISCONSIN

MADISON WISCONSIN

DISCLAIMER

This report was prepared as an account of work sponsored by an agency of the United States Government. Neither the United States Government, nor any agency thereof, nor any of their employees, makes any warranty, express or implied, or assumes any legal liability or responsibility for the accuracy, completeness, or usefulness of any information, apparatus, product, or process disclosed, or represents that its use would not infringe privately owned rights. Reference herein to any specific commercial product, process, or service by trade name, trademark, manufacturer, or otherwise, does not necessarily constitute or imply its endorsement, recommendation, or favoring by the United States Government or any agency thereof. The views and opinions of authors expressed herein do not necessarily state or reflect those of the United States Government or any agency thereof.

**Response of the National Ignition Facility
Target Chamber Walls to the Microexplosion of
a Fusion Target**

R.R. Peterson, J.J. MacFarlane, P. Wang

Fusion Technology Institute
University of Wisconsin
1500 Engineering Drive
Madison, WI 53706

<http://fti.neep.wisc.edu>

May 1994

UWFDM-952

Prepared for the Eleventh Topical Meeting on the Technology of Fusion Energy, June 19–23, 1994,
New Orleans LA.

RESPONSE OF THE NATIONAL IGNITION FACILITY TARGET CHAMBER WALLS TO THE MICROEXPLOSION OF A FUSION TARGET

Robert R. Peterson, Joseph J. MacFarlane, and Ping Wang
Fusion Technology Institute, University of Wisconsin-Madison
1500 Johnson Drive
Madison, WI 53706-1687
(608) 263-5646

ABSTRACT

The response of the National Ignition Facility target chamber first wall to the x rays and debris ions emitted by the target is important to the conceptual design of the facility. The material that is vaporized by the target emanations can condense on the laser optics, rendering them too opaque for laser transmission. This paper presents results of computer simulations of the vaporization of graphite and boron from the target chamber walls, using x-ray and debris ion spectra from target breakup simulations performed at the University of Wisconsin.

I. INTRODUCTION

The National Ignition Facility (NIF) will use a large solid state laser to drive inertial fusion targets to ignition.¹ The laser light will be converted to a wavelength of $0.35 \mu\text{m}$. The laser will direct 1.8 MJ of this light onto Hohlraum targets. The NIF will ignite inertial fusion targets with thermonuclear yields of up to 20 MJ, of which about 20% is in x rays and target debris ions. The target chamber wall is 5 m from the target, leading to a non-neutronic energy fluence of the first wall of 1.3 J/cm^2 . Depending on the coating on the first wall, material may be vaporized or melted by this energy. If the wall is coated with graphite, a very small amount of material may be vaporized. Other materials may lead to more mass loss from the wall. The target x rays reach the wall before the ions and cause the initial vaporization. If x rays constitute most of the non-neutronic energy, the ions will be absorbed in the vapor created by the x rays. The vapor will heat up and perhaps radiate enough energy to the wall to cause additional vaporization. It is important to keep the amount of material vaporized from the first wall and other structures in the target

chamber to a minimum so that laser optics do not become clouded with recondensed material. Also, the vaporization will generate a pressure on the wall that can cause vibrations or shocks in the wall. Therefore, to proceed with the design, accurate calculations of the x-ray vaporization and the secondary vaporization due to re-radiation of ion energy must be performed.

In this paper, we will present the results of simulations with the CONRAD computer code of the response of graphite and boron coated NIF target chamber first walls to x-ray and ion spectra seen from two directions.

II. NIF TARGET CHAMBER CONCEPTUAL DESIGN

The NIF target chamber is a sphere 5 m in radius. The chamber is currently thought to be filled with a very low density gas. This avoids condensation of the fill gas onto the cryogenic target. If this condensation problem can be managed at higher gas density, the vaporization of target chamber material by the target x rays and debris could be significantly reduced. The target chamber first wall is covered with plates that are coated with a material that is designed to minimize that vaporization by target emanations. Graphite and boron are considered as coating materials in this study. The properties we have assumed for the two materials are shown in Table I. For both materials, we did not have any data for the Grueneisen coefficient and assumed that it is 1.0. Graphite does not melt, but sublimates and has no melting temperature. We had no information on the true density of the plasma sprayed boron and assumed that it is 100% solid density, though this will not play a major role in these calculations. The other properties come from a number of standard references.^{2,3,8} The small

TABLE I

Properties of Graphite and Boron

	Graphite	Boron
Atomic number	6	5
Solid density (g/cm ³)	2.27	2.5
Initial density (g/cm ³)	1.80	2.5
Bulk modulus (MPa)	7900	440
Grueneisen coefficient	1.0	1.0
Lattice sep. energy (J/g)	5.98×10^4	5.69×10^4
Debye temp. (eV)	0.2137	0.1133
Melting temp. (K)	—	2573
Vaporization temp. (K)	3922	4050
Heat capacity (J/g/eV)	8240	2.67×10^4
Latent heat of Vap. (J/g)	5.973×10^4	5.69×10^4
Therm. cond. (W/cm/eV)	1.55×10^4	696

atomic number favors both materials, because the x-ray deposition lengths are long and the specific deposition is small, leading to lower surface temperatures. Comparing the two, graphite has the advantages of a higher thermal conductivity and the inability to melt; boron has a higher heat capacity and a lower atomic number. The form of these materials is under development and the properties will continue to change.

III. NIF TARGET SPECTRA

The target emissions have been calculated with the CONRAD computer code and are presented in some detail in another paper in this issue.⁴ The results are summarized in Table II. These are the results of one-dimensional spherically symmetric simulations of the breakup of the two-dimensional NIF target, which is a cylindrical gold can with a laser entrance hole in each end and a fuel capsule in the center. The “Hole” simulation models the breakup in the direction of the laser entrance hole by ignoring the effects of the gold Hohlraum case and allowing the debris and x rays from the fuel capsule to leave the target unimpeded. The “Case” simulation includes the gold Hohlraum case as a spherical shell around a capsule, which stops the debris from the capsule and converts much of the debris energy into soft x rays. The hard x rays from the capsule are attenuated by the gold case. This leads to the two time-integrated x-ray spectra shown in Fig. 1. The energy is partitioned between x rays and ions differently in the two cases because of the conversion of capsule kinetic energy into radiation by the collision between the capsule debris and the gold shell in the “Case” simulation. The debris going out the hole is also of much higher velocity and consists mostly of plastic from the ablator, while the debris

TABLE II

Results of CONRAD Simulations for the Breakup of a 20 MJ NIF Target

	Hole	Case
Total non-neutronic energy (MJ)	7.2	7.41
X-ray energy (MJ)	2.58	4.54
Debris energy (MJ)	4.60	2.87
Max. outer shell velocity (cm/ μ s)	179	35.1
Min. outer shell velocity (cm/ μ s)	101	16.2
Specific energy in debris (MJ/g)	1700	47.0

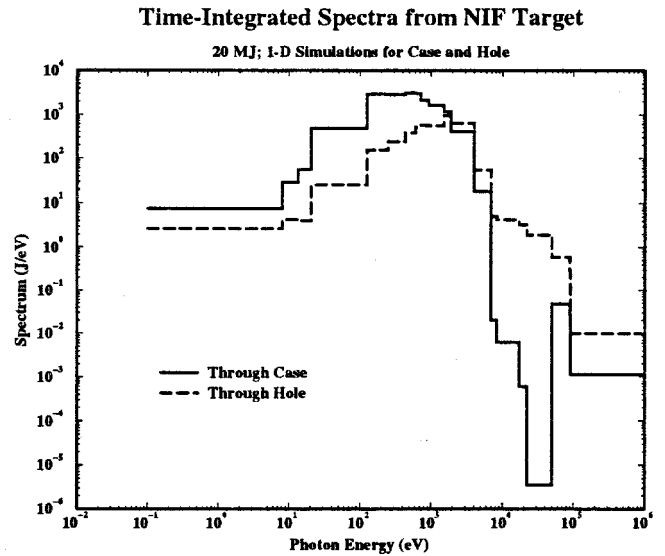


Fig. 1. Time-integrated x-ray spectra from a 20 MJ NIF target.

leaving the target in the direction of the case is mostly gold and is much slower.

Depending on the position relative to the axis of the Hohlraum, an observer sees some combination of these spectra plus a contribution from the inside of the Hohlraum case. This is illustrated in Fig. 2. If the target is observed from the region of the Inside Umbra, only the back side of the Hohlraum case can be seen and the x-ray and debris ion spectra are the “Case” values from Fig. 1 and Table II. On the Hohlraum axis, one can see the capsule through the laser entrance hole and some of the back of the case at the end of the can, so the spectra will be a mix of the “Hole” and “Case” values. Moving off the axis, the observer moves into the Capsule Penumbra and Umbra, where the capsule is first partially and then totally obscured by the case. The inside of the Hohlraum case emits x rays due to the stagnation of the capsule debris against heating the gold on the in-

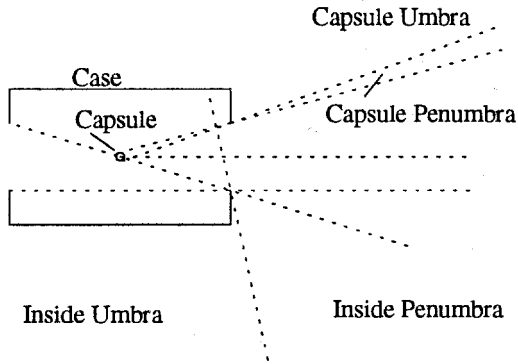


Fig. 2. Schematic picture of x-ray emission from the NIF target. The spectrum will be highly dependent on the angle the observer sits at, relative to the axis of symmetry of the target.

side of the case. This is the same as in the “Case” simulations, but the x rays are not filtered by the case. The observer sees this radiation when just off of the Hohlraum axis or in the Inside Penumbra. To test the extremes, we have performed calculations for pure “Case” and “Hole” spectra.

The temporal shapes of the x-ray and debris ion pulses on the target chamber first wall also come from the one-dimensional simulations. The x rays from the laser entrance hole have a pulse width of less than a nanosecond, while those moving through the case have a pulse width of many seconds. In both cases, the debris pulse spreads because of the velocity spread in the ions. For a 5 m propagation distance, the ions have spread to pulse widths of $2.16 \mu\text{s}$ for those from the laser entrance holes and of $16.6 \mu\text{s}$ for ions from the case.

IV. COMPUTER CODES

Simulations have been performed with the CONRAD⁵ computer code, which is a one-dimensional Lagrangian radiation-hydrodynamics code with x-ray and ion energy sources. CONRAD has been developed at the University of Wisconsin and used in several fusion plasma applications. Vaporization and condensation phenomena on a surface are modeled in the code. Radiation transport is calculated with a one-dimensional multigroup flux-limited diffusion method. Equations of state and opacities are interpolated from tables that are either supplied by the IONMIX⁶ computer code, by the EOSOPC⁷ computer code, or from the SESAME⁸ tables. CONRAD also can calculate equations-of-state internally with models that are valid at solid and higher densities using a method used in the ANEOS⁹ subroutines

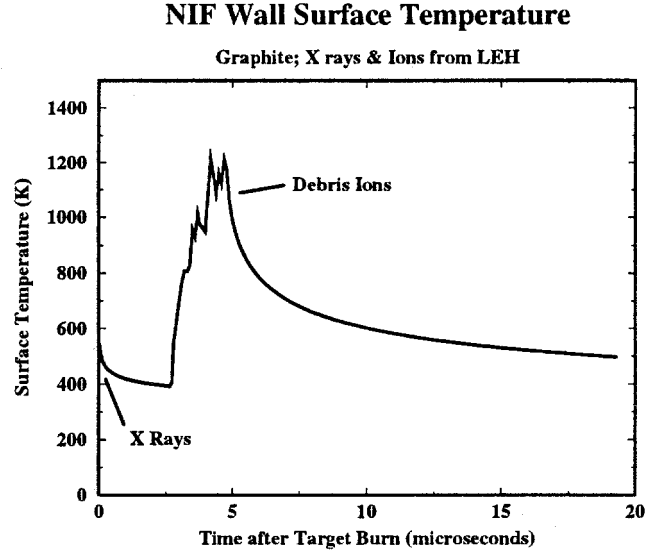


Fig. 3. Surface temperature versus time for a graphite NIF first wall irradiated by x rays and debris ions from the laser entrance hole of a 20 MJ NIF target.

used in several codes at Sandia National Laboratories. The EOSOPC code can produce opacities that are valid for high density and high atomic numbers and is used in calculation of carbon and boron opacities for the simulations discussed in this paper. The equations-of-state for these materials are calculated with the ANEOS methods that includes lattice separation energies and electron degeneracy effects, and where the material pressure is zero when the material is cold and exactly at solid density. CONRAD has a single plasma temperature, and therefore assumes that the electrons and ions are at the same temperature. Realistic time-dependent target x-ray and debris ion spectra are used. Target x-ray deposition is calculated from the cold stopping powers of Biggs and Lighthill¹⁰, with corrections to account for depletion of atomic energy levels by the x rays. Ion deposition is calculated in CONRAD with a modified Mehlhorn model¹¹ which valid to low particle energies. The charge state of the debris ions is calculated in flight. The CONRAD code has been benchmarked by comparison with laser driven shock and x-ray vaporization experiments. However, comparisons with experiments done on NOVA need to be done.

V. RESULTS

The results of simulation of the response of the target chamber wall coating to the target emissions are shown in Figs. 3, 4, 5, 6, and 7, and are summarized in Table III. Results are shown for emission

NIF Wall Temperature Profile

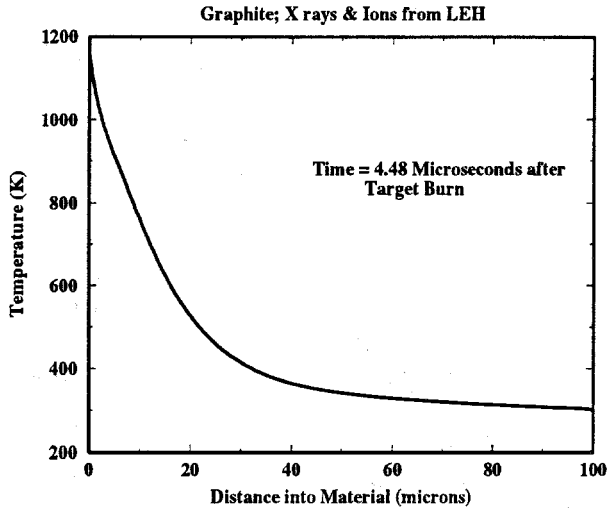


Fig. 4. Temperature profile at the time of maximum surface temperature for a graphite NIF first wall irradiated by target x rays and debris ions from the laser entrance hole of the NIF target.

from the laser entrance holes and from the Hohlraum case.

For both graphite and boron, the x rays and ions emitted from laser entrance holes do not vaporize any material. The surface temperatures are shown in Figs. 3 and 6 for graphite and boron. There is an early temperature rise due to the x rays and a later and larger rise due to the ions. In both materials, the peak temperature is well below the melting and vaporization temperatures. This is due to the wide pulse width of the debris ions on the first wall. The ion power on the surface is low enough that the material can conduct the heat away from the surface and

TABLE III

Results of CONRAD Simulations

	Hole	Case
Graphite		
Vaporized thickness (μm)	0	0.017
Total vapor* (g)	0	9.84
Peak surface temperature (K)	1260	3060
Re-radiated energy* (MJ)	0	0.74
Boron		
Vaporized thickness (μm)	0	0.003
Total vapor* (g)	0	2.21
Peak surface temperature (K)	2140	2600
Re-radiated energy* (MJ)	0	1.3

* Assuming a 5 m radius sphere.

NIF Wall Ablation

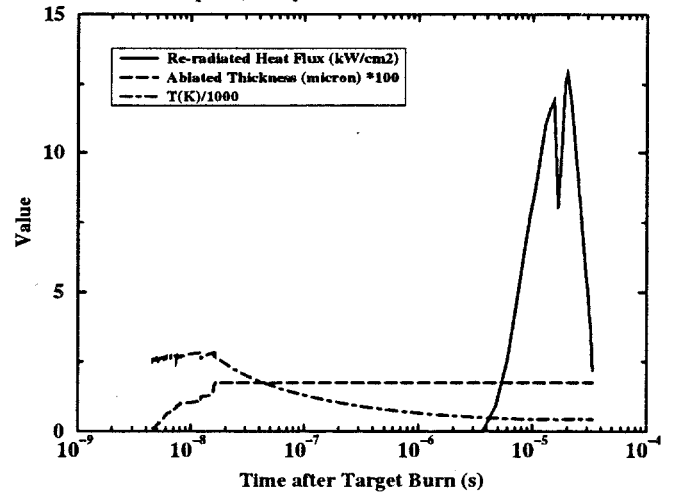


Fig. 5. Vaporized thickness versus time for a graphite NIF first wall irradiated by x-rays and debris ions from the Hohlraum case of a 20 MJ NIF target.

keep the surface temperature low. Also, the x-ray spectrum is hard enough that the deposition length is long. The temperature profile in the graphite at the time of maximum surface temperature is shown in Fig. 4, where it is seen that the surface heated layer is about $20 \mu\text{m}$ thick. This layer is susceptible to damaging thermal stresses, which could cause cracking and flaking of the surface.

The x-ray spectrum is softer for the emission from the case and vaporizes some graphite and boron from the surface. The ablated thickness, energy re-radiated by the vapor, and surface temperature are shown in Figs. 5 and 7 for graphite and boron. The x rays vaporize a small amount of graphite and boron, and the resulting vapor then absorbs the debris ions and then re-radiates the energy. In both cases, the re-radiated power is not sufficient to cause additional vaporization. In graphite, the surface temperature does not rise perceptibly because of the re-radiation, while in boron, because of its lower thermal conductivity, a small rise is seen. The mechanical impulse on the wall from the vaporization is small: 0.5 Pa-s for graphite, 2.0 Pa-s for boron.

In total, only a few grams of material are vaporized from the chamber walls; more will come from other structures. If all of the material condenses on the laser optics, which we assume to subtend 10% of the target chamber solid angle, then a $0.17 \mu\text{m}$ thick layer of graphite will be deposited on each shot. This is the worst case because some of the energy from the target will be in spectra that do not vaporize material.

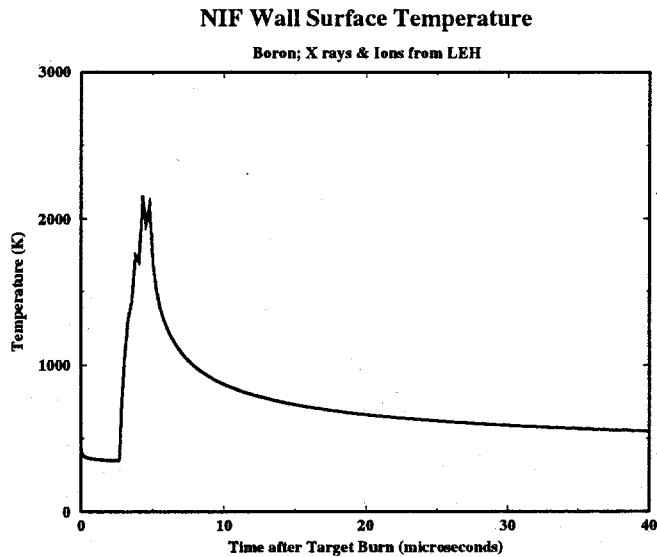


Fig. 6. Surface temperature versus time for a boron NIF first wall irradiated by x rays and debris ions from the laser entrance hole of a 20 MJ NIF target.

ACKNOWLEDGEMENT

This work is supported by the Sandia National Laboratories.

REFERENCES

1. J. A. Paisner, "Introduction to the National Ignition Facility," Workshop on the Use of the National Ignition Facility for Inertial Fusion Energy Development, Berkeley, CA, February 22-24, 1994.
2. "Handbook of Chemistry and Physics," 48th Edition, The Chemical Rubber Co. (1968).
3. "A Physicist's Desk Reference," 2nd Edition of Physics Vade Mecum, American Inst. of Physics, New York (1989).
4. Robert R. Peterson, Gregory A. Moses, Joseph J. MacFarlane, and Ping Wang, "X-Ray and Debris Ion Spectra Emanating From NIF Targets," these proceedings.
5. R. R. Peterson, J. J. MacFarlane, and G. A. Moses, "CONRAD - A Combined Hydrodynamics - Condensation/Vaporization Computer Code," University of Wisconsin Fusion Technology Institute Report UWFD-670 (January 1986, revised July 1988).

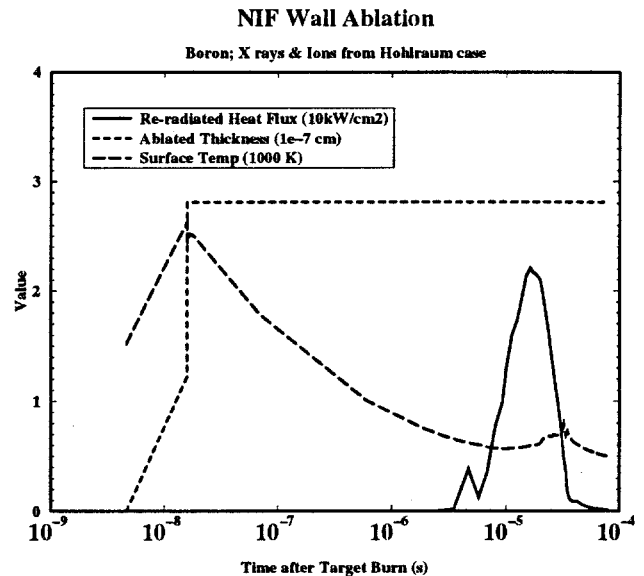


Fig. 7. Vaporized thickness versus time for a boron NIF first wall irradiated by x-rays and debris ions from the Hohlraum case of a 20 MJ NIF target.

6. J. J. MacFarlane, "IONMIX - A Code for Computing the Equation of State and Radiative Properties of LTE and Non-LTE Plasmas," *Comp. Phys. Comm.* **56**, 259 (1989).
7. Ping Wang, "EOSOPC - A Code for Computing the Equation of State and Opacities of High Temperature Plasmas with Detailed Atomic Models," University of Wisconsin Fusion Technology Institute Report UWFD-933 (December 1993).
8. B. I. Bennett, J. D. Johnson, G. I. Kerley, and G. T. Rood, "Recent Developments in the Sesame Equation-of-State Library," Los Alamos National Laboratories Report LA-7130 (February 1978).
9. S. L. Thompson and H. S. Lauson, "Improvements in the CHART D Radiation-Hydrodynamics CODE III: Revised Analytic Equations of State," Sandia National Laboratories Report SC-RR-710714 (March 1972).
10. F. Biggs, and R. Lighthill, "Analytical Approximations for X-Ray Cross Sections III," Sandia National Laboratories Report SAND-0070 (August 1988).
11. T. A. Mehlhorn, "A Finite Material Temperature Model for Ion-Driven ICF Targets," *J. Appl. Phys.* **52**, 6522 (1981).